XLI CILAMCE
XLI Ibero-Latin American Congress on Computational Methods in Engineering
16-19 November, 2020 FOZ DO IGUAÇU PARANÁ – BRAZIL

A numerical comparison between the additive and multiplicative decomposition applied to large strain thermo-elastic models

Péricles R. P. Carvalho[1], Humberto B. Coda[1], Rodolfo A. K. Sanches[1]

[1]*Dept. of Structural Engineering, São Carlos School of Engineering, University of São Paulo*
Av. Trab. São Carlense, 13566-590, São Carlos, São Paulo, Brazil
periclescarvalho@usp.br, hbcoda@sc.usp.br, rodolfo.sanches@usp.br

Abstract. In this work, we develop a numerical framework, using the finite element method, to perform two-dimensional analysis of solids with thermo-elastic constitutive model, subject to large displacements and large strains. Both the thermo-elastic model and the heat conduction equation are derived from the first and second laws of thermodynamics, where the latter is expressed by the Clausius-Duhem inequality. The formulation uses the concept of Helmholtz free energy, from which the stress and the entropy are derived. The elastic and thermal parts of deformations are distinguished by two main strategies: the additive decomposition of the Green-Lagrange strain tensor, and the multiplicative decomposition of the deformation gradient. For each, both the linear and exponential thermal expansion laws are considered, and a neo-Hookean model is applied for the elastic part. Numerical examples are proposed to show the differences and limitations of the applied models on moderate and large strain levels.

Keywords: Thermo-elasticity, Nonlinear analysis, Multiplicative decomposition, Finite Element Method

1 Introduction

The additive decomposition is already well established within the field of non-linear thermo-elasticity, as can be seen, for instance, in Holzapfel [1], Truesdell et al. [2] and Parkus [3]. The concept of multiplicative decomposition, on the other hand, emerged originally from elasto-plastic models, and was first introduced for the thermo-elastic case in Stojanović et al. [4]. The same idea was presented independently in the works of Lu and Pister [5] and Imam and Johnson [6], and since then developed and largely applied in finite deformation models (see, for instance, Mićunović [7] and Vujošević and Lubarda [8]). In this work, we present both the additive and multiplicative decompositions within a numerical scope, with the aid of the finite element method. The aim is to investigate the limitations of each model, and different thermal expansion laws, applied to cases with moderate and large strain levels. In order to do that, representative numerical examples are presented and discussed.

2 Thermo-elastic model

In this work, we apply a total Lagrangian description of the thermo-mechanical problem, i.e., we use as reference the initial undeformed configuration of the solid. Let $\mathbf{F}$ denote the deformation gradient from the initial to the deformed configuration. Then, the Green-Lagrange strain is given by $\mathbf{E} = \frac{1}{2}(\mathbf{F}^T\mathbf{F} - \mathbf{I})$, where $\mathbf{I}$ is the second order identity tensor. The work-conjugate of $\mathbf{E}$ is the Second Piola-Kirchhoff Stress, denoted here by $\mathbf{S}$.

The first and second laws of thermodynamics form the basis for a thermodynamically-based constitutive model. The first, also known as law of conservation of energy, can be written, using the principle of rate of work, as

$$\dot{\psi} + \rho_0 \left(T\dot{\eta} + \dot{T}\eta - R \right) = \mathbf{S} : \dot{\mathbf{E}} - \boldsymbol{\nabla}_0 \cdot \mathbf{q}_0, \tag{1}$$

where ψ denotes the Helmholtz free energy (per unit volume in the initial configuration), ρ_0 the density in the initial configuration, T the temperature, η the entropy per unity mass, R the internal heat produced per unit time and unit mass, $\mathbf{q}_0$ the heat flux in the initial configuration, and $\boldsymbol{\nabla}_0$ the gradient vector in the initial configuration.

As for the second law of thermodynamics, it can be written in the form of the Clausius-Duhem inequality, which gives

$$\mathbf{S} : \dot{\mathbf{E}} - \dot{\psi} - \rho_0 \dot{T}\eta - \frac{1}{T}\mathbf{q}_0 \cdot \boldsymbol{\nabla}_0 T \geq 0. \tag{2}$$

For thermo-elastic models, the Helmholtz free energy can be written entirely in terms of the Green-Lagrange strain ($\mathbf{E}$) and the temperature (T), which means the rate of the Helmholtz free energy can be written as

$$\dot{\psi} = \frac{\partial \psi}{\partial \mathbf{E}} : \dot{\mathbf{E}} + \frac{\partial \psi}{\partial T}\dot{T}, \tag{3}$$

and therefore the first and second laws of thermodynamics can be rewritten as

$$\left(\mathbf{S} - \frac{\partial \psi}{\partial \mathbf{E}}\right) : \dot{\mathbf{E}} - \left(\frac{\partial \psi}{\partial T} + \rho_0 \eta\right)\dot{T} + \rho_0 \left(R - T\dot{\eta}\right) - \boldsymbol{\nabla}_0 \cdot \mathbf{q}_0 = 0, \tag{4}$$

$$\left(\mathbf{S} - \frac{\partial \psi}{\partial \mathbf{E}}\right) : \dot{\mathbf{E}} - \left(\frac{\partial \psi}{\partial T} + \rho_0 \eta\right)\dot{T} - \frac{1}{T}\mathbf{q}_0 \cdot \boldsymbol{\nabla}_0 T \geq 0. \tag{5}$$

Since these relations must the fulfilled for arbitrary thermodynamic processes, i.e., arbitrary values of $\dot{\mathbf{E}}$ and $\dot{T}$, it follows that:

$$\mathbf{S} = \frac{\partial \psi}{\partial \mathbf{E}}, \qquad \eta = -\frac{1}{\rho_0}\frac{\partial \psi}{\partial T}, \qquad \rho_0 \left(R - T\dot{\eta}\right) - \boldsymbol{\nabla}_0 \cdot \mathbf{q}_0 = 0 \qquad \text{and} \qquad \frac{1}{T}\mathbf{q}_0 \cdot \boldsymbol{\nabla}_0 T \leq 0. \tag{6}$$

The first two equations are the constitutive relations, and the third is the equation of heat conduction. For the constitutive equations, it may be convenient to decompose the Helmholtz free energy additively into a mechanical part, denoted as ψ_m, and a thermal part, denoted as ψ_t. The later depends only on the temperature, while ψ_m depends only on the mechanical strain. However, the way in which the mechanical strain is obtained will depend on the type of decomposition applied, as discussed in the next subsections.

2.1 Additive decomposition

In linear thermo-elasticity, one of the most commonly adopted models is based on the additive decomposition of the engineering strain into a mechanical and a thermal component. For the non-linear case, an usual generalization of this concept is the additive decomposition of the Green-Lagrange strain:

$$\mathbf{E} = \mathbf{E}_m + \mathbf{E}_t \tag{7}$$

in which $\mathbf{E}_m$ represents the mechanical parcel, associated with the constitutive law, and $\mathbf{E}_t$ represents the thermal parcel, associated with a thermal expansion law. In this work, we apply the linear and exponential expansion laws, given, respectively, by

$$\lambda_t = 1 + \alpha(T - T_0), \quad \text{and} \tag{8}$$

$$\lambda_t = e^{\alpha(T - T_0)} \tag{9}$$

where λ_t is the thermal stretch ratio, α is the thermal expansion coefficient of the material, and T_0 is the reference temperature. For isotropic materials, $\mathbf{E}_t$ can be calculated by the relation $\mathbf{E}_t = \frac{1}{2}(\lambda_t^2 - 1)\mathbf{I}$, in which $\mathbf{I}$ is the identity tensor.

In order to account for large strain problems, a neo-Hookean constitutive model is applied in this work. The mechanical component of the Helmholtz free energy in the initial configuration is written as

$$\psi_m = \frac{\Lambda}{2}\ln J_m + G\left(\operatorname{tr}\mathbf{C}_m - 3 - \ln J_m\right), \tag{10}$$

where Λ and G are the Lamé parameters, which can be calculated from the Young's Modulus (E) and the Poisson's ratio (ν), $\mathbf{C}_m = 2\mathbf{E}_m + \mathbf{I}$ is the mechanical right Cauchy-Green deformation tensor, and $J_m = \sqrt{\det \mathbf{C}_m}$ is the mechanical Jacobian (or volumetric strain). By using eq. (10) and applying the kinematic relation from eq. (7), the Second Piola-Kirchhoff stress for this model is given by:

$$\mathbf{S} = \frac{\partial \psi_m}{\partial \mathbf{E}} = \frac{\partial \psi_m}{\partial \mathbf{E}_m} : \cancel{\frac{\partial \mathbf{E}_m}{\partial \mathbf{E}}} = \frac{\partial \psi_m}{\partial \mathbf{E}_m} = \Lambda(\ln J_m)\mathbf{C}_m^{-1} + G(\mathbf{I} - \mathbf{C}_m^{-1}). \tag{11}$$

2.2 Multiplicative decomposition

The multiplicative decomposition is based on the existence of an intermediate configuration Ω_t, in which only thermal strains are present. From this, we denote by $\mathbf{F}_t$ the thermal deformation gradient, mapping from the initial configuration to Ω_t, and by $\mathbf{F}_m$ the mechanical deformation gradient, mapping from Ω_t to the deformed configuration. Thus, by a simple composition of functions, one concludes that the total deformation gradient is given by $\mathbf{F} = \mathbf{F}_m\mathbf{F}_t$. For isotropic materials, however, $\mathbf{F}_t = \lambda_t\mathbf{I}$, i.e., the multiplicative decomposition can be written simply as

$$\mathbf{F} = \lambda_t\mathbf{F}_m, \tag{12}$$

which results in the following kinematic relations:

$$\mathbf{E}_m = \frac{1}{2}(\mathbf{F}_m^T\mathbf{F}_m - \mathbf{I}) = \lambda_t^{-2}\mathbf{E} + \frac{1}{2}(\lambda_t^{-2} - 1)\mathbf{I} = \lambda_t^{-2}(\mathbf{E} - \mathbf{E}_t). \tag{13}$$

Analogously to the previous model, the thermal stretch ratio λ_t can be given both by a linear or an exponential thermal expansion law (eqs. (8) and (9), respectively). As can be noted from eq. (13), for infinitely small thermal deformations (i.e., $\lambda_t \approx 1$), the multiplicative decomposition is approximately equivalent to the additive.

An important remark of the multiplicative decomposition is the fact that the elastic constitutive law is defined in the intermediate configuration instead of the initial configuration. Therefore, in order to be consistent with the total Lagrangian framework previously discussed, one must take into account the volumetric deformations between the initial and intermediate configurations (see Vujošević and Lubarda [8]). With that in mind, the mechanical Helmholtz free energy is now written as

$$\psi_m = \lambda_t^3\left[\frac{\Lambda}{2}\ln J_m + G\left(\operatorname{tr}\mathbf{C}_m - 3 - \ln J_m\right)\right]. \tag{14}$$

By deriving eq. (14) and using the kinematic relation given in eq. (13), the Second Piola-Kirchhoff stress is given by

$$\mathbf{S} = \frac{\partial\psi_m}{\partial\mathbf{E}_m} : \frac{\partial\mathbf{E}_m}{\partial\mathbf{E}} = \frac{\partial\psi_m}{\partial\mathbf{E}_m}\lambda_t^{-2} = \lambda_t\left[\Lambda(\ln J_m)\mathbf{C}_m^{-1} + G(\mathbf{I} - \mathbf{C}_m^{-1})\right]. \tag{15}$$

3 Equation of heat conduction

Let $c_E = \rho_0 T\frac{\partial\eta}{\partial T}$ be the specific heat capacity of the material per unit volume in the initial configuration, and $\mathcal{C}_{te} = \rho_0\frac{\partial\eta}{\partial\mathbf{E}}$. Then, the equation of heat conduction, introduced in eq. (6), can be rewritten as

$$\boldsymbol{\nabla}_0\cdot\mathbf{q}_0 + T\mathcal{C}_{te} : \dot{\mathbf{E}} + c_E\dot{T} = \rho_0 R. \tag{16}$$

In most materials, the term $T\mathcal{C}_{te} : \dot{\mathbf{E}}$ has a much lower order of magnitude when compared with the other terms, and therefore it will be neglected in this work. We also assume that c_E is a constant parameter, which can be achieved by setting an appropriate expression for ψ_t.

The relation between heatflux and temperature is given by the Fourier's law, $\mathbf{q} = -k\cdot\boldsymbol{\nabla}T$, where k is the thermal conductivity parameter, and $\boldsymbol{\nabla}T$ is the gradient of temperature in the deformed configuration. We note that, in this context, $\mathbf{q}$ is given in its Eulerian form, i.e., taking as reference the deformed configuration. However, it can be related to $\mathbf{q}_0$ by the equation $\mathbf{q}_0 = (\det\mathbf{F})\mathbf{F}^{-1}\cdot\mathbf{q}$. After integrating eq. (16) in the initial volume, multiplying by a variation of temperature δT, performing certain algebraic manipulations, and applying the Fourier's law, the equation of heat conduction can be written in the following global variational form:

$$\int_{\Omega_0}(\mathbf{K}_0\cdot\boldsymbol{\nabla}_0 T)\cdot(\boldsymbol{\nabla}_0\delta T)dV_0 + \int_{\Omega_0} c_E\dot{T}\delta T dV_0 + \int_{\Gamma_0}\bar{q}_0\delta T dS_0 - \int_{\Omega_0}\rho_0 R\delta T dV_0 = 0 \tag{17}$$

where $\mathbf{K}_0 = k(\det\mathbf{F})\mathbf{C}^{-1}$ is the Lagrangian conductivity matrix, Ω_0 is the initial volume of the solid, and $\bar{q}_0$ is a prescribed heatflux in the boundary Γ_0. Equation (17) is solved in this work by the finite element method. A more detailed description of the heat transfer problem applied to FEM can be seen, for instance, in Dhondt and Sons [9].

4 Numerical examples

For the numerical implementation of the model, the mechanical and thermal problems are solved independently and coupled iteratively by a strong partitioned approach (see Matthies et al. [10]). The mechanical problem is solved by a position based finite element method, where geometrical and physical non-linearities are considered (see Coda [11], Coda and Paccola [12] and Sanches and Coda [13] for more details). The same finite element discretization is used to solve the heat conduction equations.

4.1 Isostatic beam under thermal and mechanical loads

In this example, we consider a bi-supported beam with geometry, mesh and parameters presented in Fig. 1. This beam is subject to variations of temperature $-\Delta T$ and ΔT in the upper and lower boundaries, respectively, and an uniformly distributed mechanical load p. Two different analysis are considered for this example: in the first, only the thermal loads are applied, i.e., $p = 0$, and $\Delta T = 25°\text{C}$. In the second analysis, we apply a mechanical load $p = 2$ kN/m^2 and a variation of temperature $\Delta T = 15°\text{C}$. For both cases, the additive and multiplicative decompositions, as well as the linear and exponential thermal expansion laws, are considered.

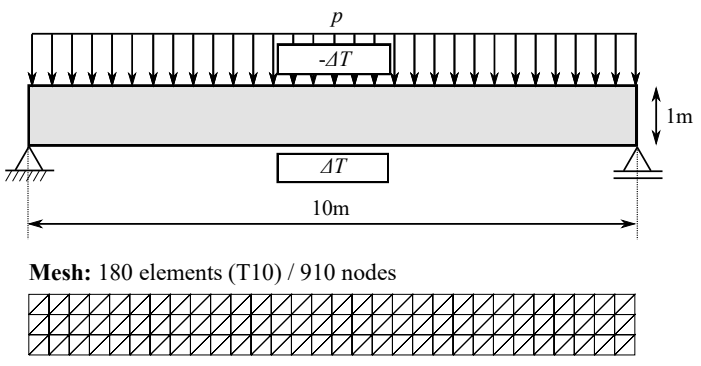

Analysis parameters:
- Steady state ($c_E = 0$)
- Static analysis
- 100 step, with ΔT and p evolving linearly

Thermal parameters:
- $k = 10^3$ W/(m ºC)
- $\alpha = 0.01$ /ºC

Mechanical parameters:
- Neo-Hookean/Plane stress
- $E = 1000$ kN/m^2
- $\nu = 0.4$

Figure 1. Geometry, mesh and parameters for the beam under thermal and mechanical loads example

The final deformed configuration for all cases considered are shown in Fig. 2. As expected from a isostatic structure, the first case (purely thermal load) results in no reaction forces. However, one can still notice self-balanced residual stresses due to incompatibilities between the displacements and purely thermal deformations, which can be seen mostly in the cases where a linear thermal expansion law is applied. The exponential law, on the other hand, provides a better compatibility in this regard, since the resulting residual stresses are negligible. Finally, for the second analysis case, also shown in Fig. 2, not only the deforming behavior is different, but the stress values are more significant than the previous case, due to the introduction of mechanical forces.

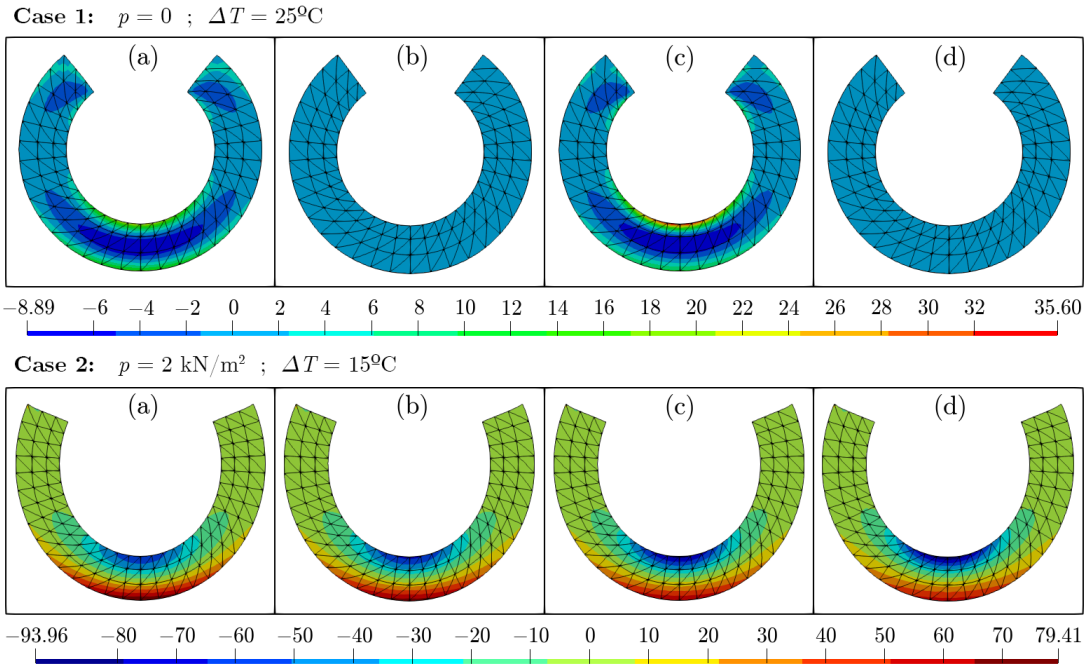

Figure 2. Final deformed configuration of the beam example for two different load cases, with component σ_{11} of Cauchy stress displayed in color map. (a) Additive decomposition with linear thermal expansion law; (b) Additive decomposition with exponential law; (c) Multiplicative decomposition with linear law and (d) Multiplicative decomposition with exponential law.

In Fig. 3 we show the evolution of the vertical displacement and horizontal component of Green-Lagrange strain (E_{11}), both in the middle point of the beam's lower boundary. For the purely thermal load case, there are no significant differences between the additive and multiplicative decompositions, since the mechanical deformations are residual, i.e., the total deformations are mostly thermal for this case. However, major differences between the linear and exponential expansion laws can be seen in this case, specially in the strain graph. The opposite can be noted in the second analysis case: since the thermal deformations are smaller, the difference between the expansion laws is less evident. However, as consequence of the introduction of mechanical forces, the mechanical strain is in the same order of magnitude as the thermal strain, and therefore the role of the choice of decomposition is more significant, as can be seen mainly in the strain results.

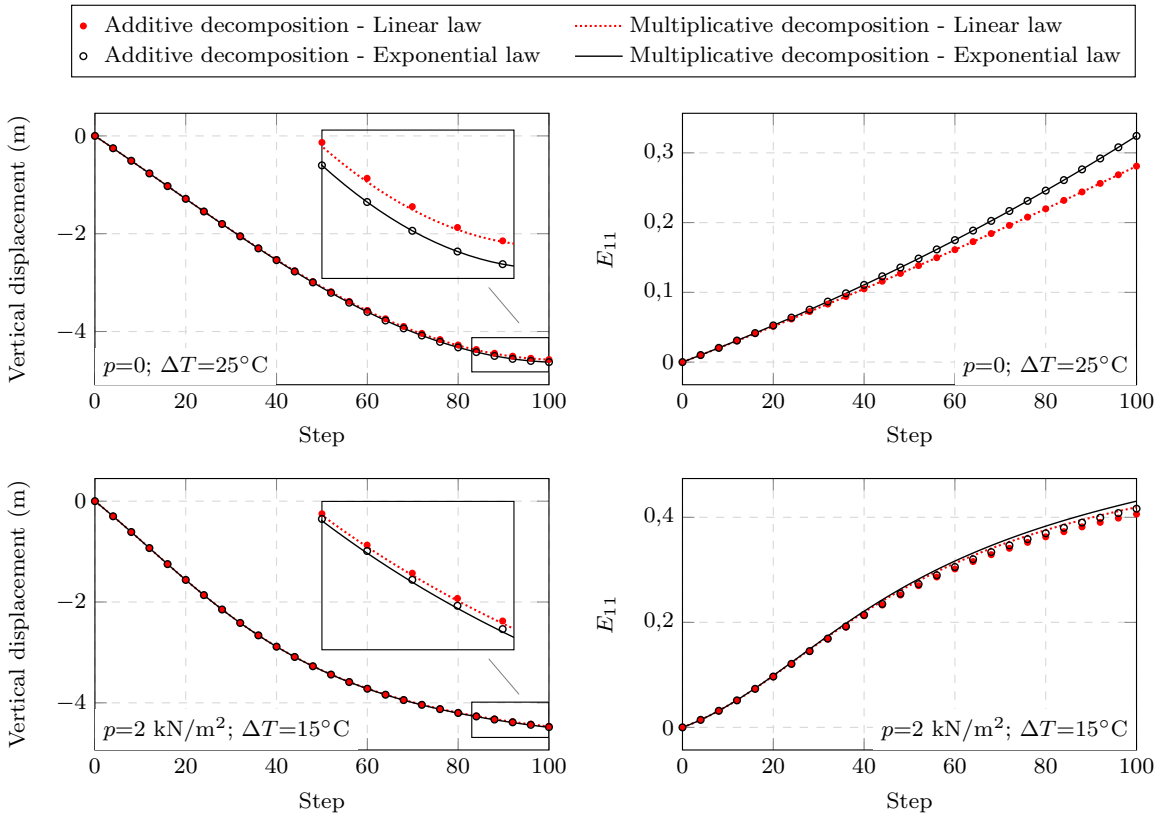

Figure 3. Evolution of vertical displacement and component E_{11} of Green-Lagrange strain for the beam example

4.2 Large deformation cube

In this section, a large deformation example is proposed to better evidence the relevance of the proper choice of decomposition. It consists of an overheated cube, initially at 600°C, subject to heat transfer with the ambient (at 25°C) via convection (see Fig. 4). The convection is applied as precribed heatflux, using Newton's law of cooling: $\bar{q} = h(T - T_{ext})$, where h is the heat transfer coefficient, and T_{ext} is the temperature of the ambient.

Again, both the additive and multiplicative decompositions are applied, together with linear and exponential thermal expansion laws. However, in the cases where additive decomposition or linear law are applied, the high compressive strains resulted in negative Jacobian at given points of the analysis, causing convergence problems. For the case with additive decomposition and linear law, the error occurred in step 11 ($t = 2.75$ s); For the case with additive decomposition and exponential law, in step 34 ($t = 8.5$ s); and for the multiplicative decomposition with linear law, in step 151 ($t = 37.75$ s). The only case where no errors occurred was the one with multiplicative decomposition and exponential law, which, as expected, is more suitable for problems with large compressive strains. The results for each analysis are shown in Fig. 5 up to the step with convergence problem. The deformed configurations for the case with multiplicative decomposition and exponential law are shown in Fig. 6, together with the values of the horizontal component of Cauchy stress (σ_{11}).

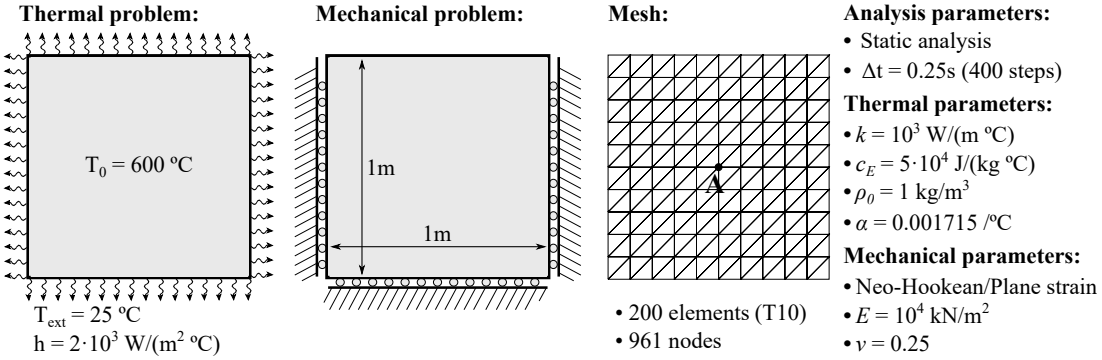

Figure 4. Geometry, mesh and parameters for the large deformation cube example

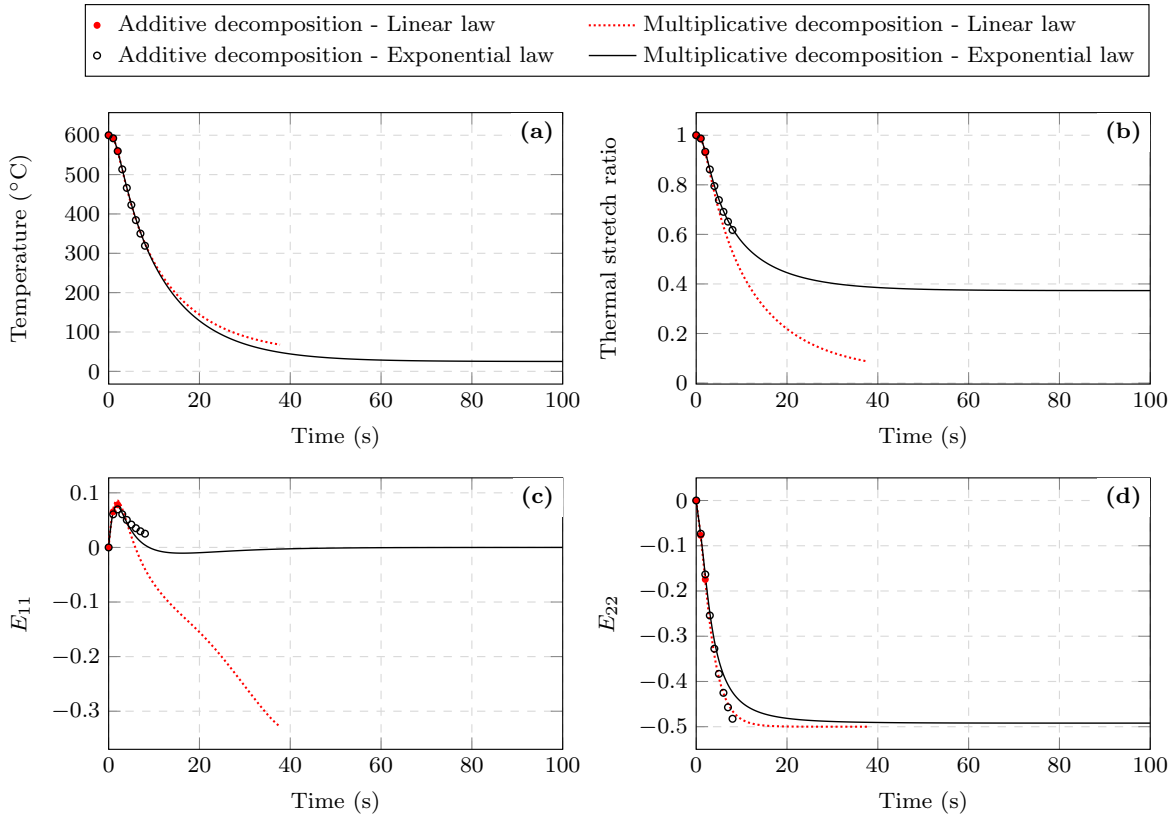

Figure 5. Evolution of (a) temperature, (b) thermal stretch ratio, (c) E_{11} and (d) E_{22} at the point A, for the large deformation cube example

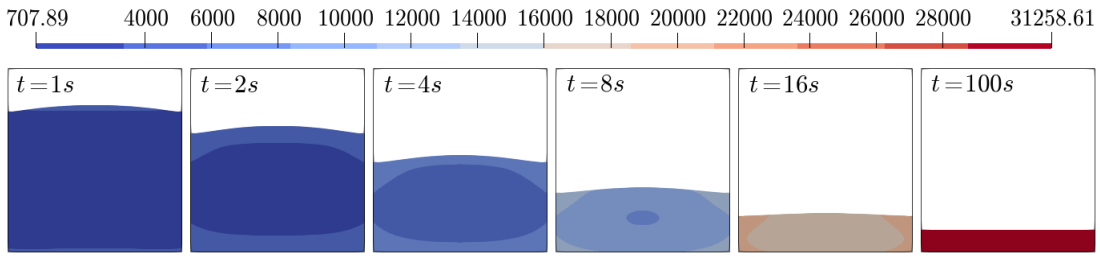

Figure 6. Deformed configurations for the large deformation cube example, using the multiplicative decomposition and exponential thermal expansion law, with component σ_{11} of the Cauchy stress displayed in the color map

5 Conclusions

The proposed numerical examples were able to show the main differences between the four thermo-elastic models presented in this work. As could be seen from the isostatic beam example (section 4.1), the models are approximately equivalent while in the small strain regime, but tend to divert from each other in moderate strain levels. The difference between the additive and multiplicative decomposition, however, is only significant for the case where mechanical and thermal strains are in the same order of magnitude (second analysis case). As for the case with purely thermal loads, the difference lies basically in the adopted thermal expansion law. A remarkable difference in this case is the fact that the exponential law is free from residual stresses, as opposite to the linear law. For the next example (section 4.2), the models were applied to a case with excessively large strain levels. As expected, the models with linear expansion law or additive decomposition proved to be inappropriate for this analysis, showing convergence problems in early steps due to negative Jacobian. The case with multiplicative decomposition and exponential law, however, showed no convergence problem during the analysis, leading to the conclusion that, from the presented models, it is the most appropriate for large strain problems.

Acknowledgements. This study was financed in part by the *Coordenação de Aperfeiçoamento de Pessoal de Nível Superior – Brasil* (CAPES) – Finance Code 001 –, the Brazilian agency National Council for Scientific and Technological Development (CNPq) – grant 310482/2016-0 – , and the São Paulo Research Foundation (FAPESP) – Process Number 2018/23957-2. The authors would like to thank them for the financial support given to this research.

Authorship statement. The authors hereby confirm that they are the sole liable persons responsible for the authorship of this work, and that all material that has been herein included as part of the present paper is either the property (and authorship) of the authors, or has the permission of the owners to be included here.

References

[1] Holzapfel, G., 2000. *Nonlinear Solid Mechanics: A Continuum Approach for Engineering*. Wiley.
[2] Truesdell, C., Truesdell, C., Noll, W., Antman, S., & Noll, W., 2004. *The Non-Linear Field Theories of Mechanics*. Number v. 3 in The non-linear field theories of mechanics. Springer.
[3] Parkus, H., 2012. *Thermoelasticity*. Springer Vienna.
[4] Stojanović, R., Djurić, S., & Vujosević, L., 1964. On finite thermal deformations. *Archiwum Mechaniki Stosowanej*, vol. 1, n. 16, pp. 103–108.
[5] Lu, S. & Pister, K., 1975. Decomposition of deformation and representation of the free energy function for isotropic thermoelastic solids. *International Journal of Solids and Structures*, vol. 11, n. 7, pp. 927 – 934.
[6] Imam, A. & Johnson, G. C., 1998. Decomposition of the Deformation Gradient in Thermoelasticity. *Journal of Applied Mechanics*, vol. 65, n. 2, pp. 362–366.
[7] Mićunović, M., 1974. A geometrical treatment of thermoelasticity of simple inhomogeneous bodies. i: Geometrical and kinematical relations. *Bulletin de l'Académie Polonaise des Sciences, Série des Sciences Techniques*, vol. 22.
[8] Vujošević, L. & Lubarda, V., 2002. Finite-strain thermoelasticity based on multiplicative decomposition of deformation gradient. *Theoretical and applied mechanics*, , n. 28-29, pp. 379–399.
[9] Dhondt, G. & Sons, J. W. ., 2004. *The Finite Element Method for Three-Dimensional Thermomechanical Applications*. Titolo collana. Wiley.
[10] Matthies, H. G., Niekamp, R., & Steindorf, J., 2006. Algorithms for strong coupling procedures. *Computer Methods in Applied Mechanics and Engineering*, vol. 195, n. 17, pp. 2028 – 2049. Fluid-Structure Interaction.
[11] Coda, H. B., 2018. *O Método dos elementos finitos posicional*. EESC/USP, São Carlos.
[12] Coda, H. B. & Paccola, R. R., 2007. An alternative positional FEM formulation for geometrically nonlinear analysis of shells: Curved triangular isoparametric elements. *Computational Mechanics*, vol. 40, n. 1, pp. 185–200.
[13] Sanches, R. A. & Coda, H. B., 2013. Unconstrained vector nonlinear dynamic shell formulation applied to fluid structure interaction. *Computer Methods in Applied Mechanics and Engineering*, vol. 259, pp. 177 – 196.